# Composite carbon-based ionic liquid supercapacitor for high-current micro devices

**M Cowell[1], R Winslow[1], Q Zhang[2], J Ju[1], J Evans[2] and P Wright[1]**

[1]Department of Mechanical Engineering, University of California at Berkeley, 6141 Etcheverry Hall, Berkeley CA, 94709 USA

[2]Department of Materials Science and Engineering, University of California at Berkeley, 210 Hearst Mining Building, Berkeley CA, 94720 USA

E-mail: martin.cowell@berkeley.edu

**Abstract.** Manufacture and performance of a composite carbon-based supercapacitor that employs a gel polymer ionic liquid electrolyte to achieve stable, long cycle life, high-current draw energy storage is discussed in this paper. This supercapacitor when cycled galvanostatically can achieve a discharge capacitance of 43.0 mF per square centimeter of substrate by leveraging the strengths of a composite electrode composition. The printed manufacturing process takes place in ambient conditions at room temperature enabling high-current, rechargeable energy storage to be built onto many substrates. Single-cell discharge power densities have reached 404 $\mu$W/cm$^2$, which could enable many technologies when paired with a MEMS energy harvester.

## 1. Introduction

Powering high-current micro devices with low power generation often found at the micro-scale [1] requires that energy be trickle-charged into a storage device capable of high-current discharge. While arrays of micro piezoelectric vibrational energy harvesters have been used to increase system output power [2], the power required to energize a wireless radio is still much higher [3]. Charge storage via an electric double layer, such as found in a supercapacitor, offers high-current discharging while maintaining long cycle-life performance. The thermal and chemical stability of the ionic liquid electrolyte 1-butyl-3-methylimidazolium tetrafluoroborate ([BMIM+][BF4-]) allows the thick film capacitor to be employed in harsh environments where aqueous electrolytes would otherwise evaporate [4], while the polymer binder allows for structural flexibility.

Experimental testing reached a maximum voltage of 1.0 V and achieved a discharge efficiency of 84.2%, discharge power of 404 $\mu$W/cm$^2$, and discharge energy of 5.03 $\mu$W-hr/cm$^2$. Long cycle life testing of up to 100,000 cycles showed no sign of precipitous cell degradation.

Previous work confirmed a proof of concept for the printability of carbon based ionic liquid supercapacitors but left composition optimization and manufacturing process control unfinished. The research presented in this paper improves upon the proof of concept with a composite carbon electrode to achieve higher capacitance, energy, and power density.

## 2. Cell Manufacturing

### *2.1. Layer Composition*

Symmetrical capacitor geometry was employed with dry electrodes composed of activated carbon (AC), acetylene black (AB), graphite (GR), and poly(vinylidene fluoride-co-

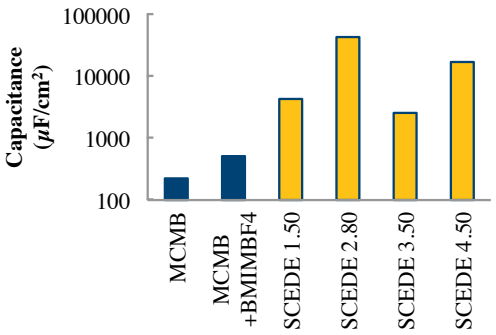


**Figure 1.** Capacitance performance improvements over previous work by leveraging AC, AB, and GR.

**Table 1.** Composite electrode variations. NMP was used to achieve rheology suitable for printing.

| Composite Electrode Version | Electrode Composition AC:AB:GR:PVDF-HFP (Mass Ratio) |
|---|---|
| 1.50 | 0:1:0:1 |
| 2.50 | 1:0:1:2 |
| 2.80 | 2:0:2:1 |
| 3.50 | 0:9:1:10 |
| 4.50 | 17:1:2:20 |

hexafluoropropylene) (PVDF-HFP) with mass ratios outlined in table 1. Previous work by our lab used mesocarbon microbeads (MCMB) and AB as active electrode materials [5], but these have been found to have an average capacitance of 0.50 mF/cm$^2$ as seen in figure 1. To improve capacitance performance, composite electrodes leverage the high surface area of AC with the electrically conductive microstructure of AB [6] and structural reinforcement of GR. The solvent n-methylpyrrolidone (NMP) was used to suspend the active material and solvate the polymer binder to achieve favorable rheological properties for printed manufacturing.

The gel polymer electrolyte (GPE) was composed of (50 wt%) PVDF-HFP and (50 wt%) [BMIM+][BF4-]. NMP was also used as a solvent to ensure a printable rheology. The gel polymer layer electrically separated the electrodes while contributing ion migration pathways to support the electric double layer characteristic of supercapacitors.

### *2.2. Layer Dispenser Printing and Assembly*

The electrolyte was printed via CNC pneumatic dispenser printer, and electrodes were stencil cast (figure 2). They were dried in an oven at 80°C for 12 hours, driving off the NMP to leave only the active and binder materials. Once dry, electrodes were peeled off their stainless steel substrate without damaging their structural integrity. Dried gel polymer electrolyte layers were peeled off their glass substrate (figure 3). The dry layers were wetted with [BMIM+][BF4-] and stacked to create parallel-opposed cells (figure 4), which were housed in CR2023 coin cells for cycling and performance characterization.

## 3. Testing and Performance Results

Short cycle galvanostatic testing was performed on the Gamry Reference 600$^{TM}$. Constant current charge and discharge cycling was performed as outlined in supercapacitor testing standard IEC 62391-1:2006 [7]. During this cycling regime supercapacitors were looped ten times through steps outlined in table 2.

Energy was quantified via numerical integration of the voltage-current product vs. time curve during charging and discharging described by

$$W = \sum_{t=t_o}^{t_f} I_t V_t \Delta t \tag{1}$$

where $I_t$ is the time series current in amperes, $V_t$ is the time series voltage in volts, $\Delta$t is the time step between samples in seconds, $t_f$ and $t_o$ are the final time and initial time in seconds.

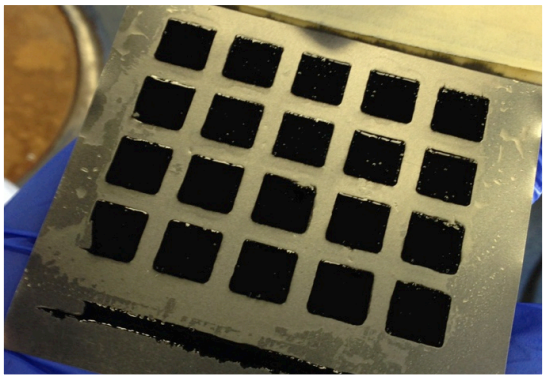

**Figure 2.** Stencil cast electrodes before drying.

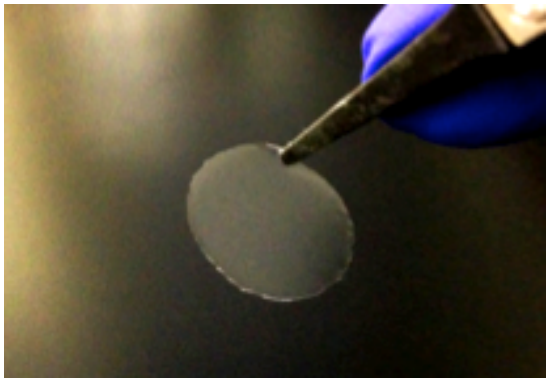

**Figure 3.** Gel polymer ionic liquid electrolyte after oven drying.

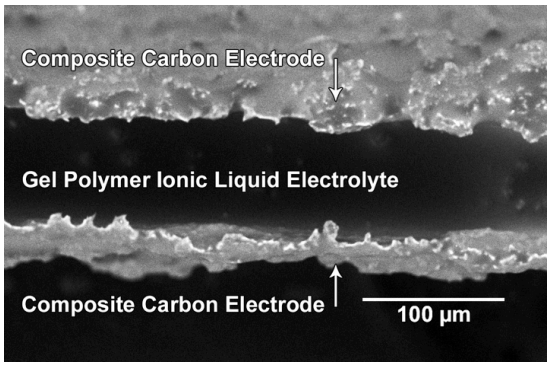


**Figure 4.** SEM of stacked cross section of carbon electrode and GPE.

**Table 2.** Constant current charge and discharge regime.

| Step Name | Limit/ Condition |
|---|---|
| Constant current charge | 1.00 V |
| Rest | 5.00 s |
| Constant current discharge | 0.00 V |
| Rest | 5.00 s |

Power during charge and discharge was quantified by

$$P = W/(t_f - t_o) \tag{2}$$

Bulk capacitance was calculated using the time rate of change of voltage relation between current and capacitance, based on states at the beginning and end of charge and discharge:

$$C = I(t_f - t_o)/(V_f - V_o) \tag{3}$$

where I is the average current in amperes, $V_f$ is the voltage at the end of the charge or discharge step, and $V_o$ is the voltage at the start of the charge or discharge step.

Equivalent series resistance (ESR) was calculated using Ohm's law for voltage drop seen at the transition between charge, rest, and discharge steps:

$$ESR = (V_{o-1} - V_o)/I \tag{4}$$

where $V_{o-1}$ represents the voltage immediately before charging or discharging begins. The voltage drop across the cell becomes substantial at higher discharge rates.

Coulombic efficiency was defined as

$$\eta_C = \sum_{t=t_o}^{t_f Discharge} I_t \Delta t / \sum_{t=t_o}^{t_f Charge} I_t \Delta t \tag{5}$$

where the number of coulombs transferred was determined through numerical integration of current-time series data.

Energy efficiency was defined as

$$\eta_E = W_d/W_c \tag{6}$$

where $W_d$ represents the discharge energy in joules and $W_c$ represents charge energy in joules.

Figures 5 and 6 show data taken from a cell whose electrodes (1 cm x 1 cm each) were composed of composition 2.80 and separated by a single layer of GPE 60 $\mu$m thick. The cell was subjected to constant current charge/discharge regimes using the same magnitude of current during charging and discharging steps (10 and 1000 $\mu$A/cm$^2$ for the two tests). The high voltage limit of 1.0 V was selected to avoid the possibility of side reactions associated with the electrolysis of trace water, but the cells were expected to be able to sustain voltages of 2.5 V to 4.0 V without breakdown of the ionic liquid electrolyte [8]. Results from the two tests are shown in table 3. Performance metrics were normalized by a footprint area of 1 cm$^2$.

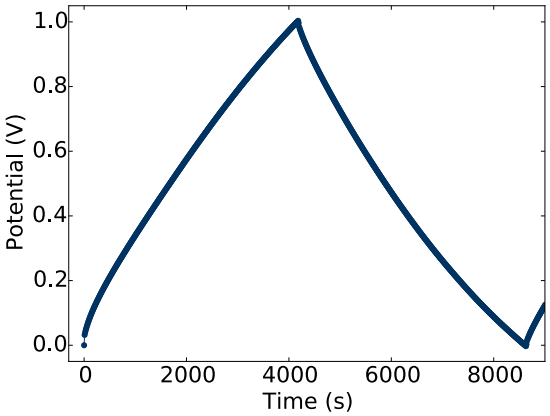


**Figure 5.** Constant current (10 $\mu$A/cm$^2$) charge/discharge voltage response of supercapacitor cell using electrode composition 2.80.

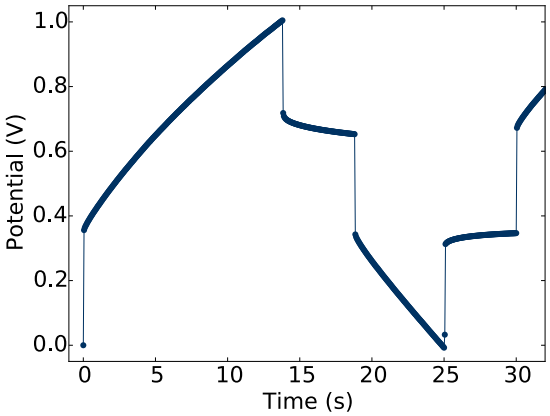


**Figure 6.** Constant current (1000 $\mu$A/cm$^2$) charge/discharge voltage response of supercapacitor cell using electrode composition 2.80.

**Table 3.** Performance metrics of supercapacitor cell containing electrode 2.80 tested at two different current densities.

| | 10 $\mu$A/cm$^2$ | | 1000 $\mu$A/cm$^2$ | |
|---|---|---|---|---|
| | Charge | Discharge | Charge | Discharge |
| Energy ($\mu$W-hr/cm$^2$) | 6.75 | 5.03 | 1.61 | 0.300 |
| Power ($\mu$W/cm$^2$) | 5.46 | 4.26 | 855 | 164 |
| Capacitance (mF/cm$^2$) | 45.0 | 43.0 | 20.4 | 18.0 |
| ESR ($\Omega$) | 1020 | 1150 | 325 | 307 |
| Coulombic Efficiency (%) | 95.4 | | 97.5 | |
| Energy Efficiency (%) | 74.4 | | 18.7 | |

As is evident in table 3, the testing regime heavily influenced the performance of the supercapacitor cell. The highest reported discharge energy density (5.03 $\mu$W-hr/cm$^2$) and discharge capacitance density (43.0 mF/cm$^2$) were attained by composition 2.80 at a discharge

current of 10 $\mu$A/cm$^2$; discharge power density (404 $\mu$W/cm$^2$), composition 1.50 at 1000 $\mu$A/cm$^2$; lowest reported discharge ESR (79.0 ohms), composition 2.50 at 1000 $\mu$A/cm$^2$; highest reported coulombic efficiency (100%), composition 3.50 at 1000 $\mu$A/cm$^2$; and highest reported energy efficiency (84.2%), composition 1.50 at 50 $\mu$A/cm$^2$. (Please note the 100% coulombic efficiency is accurate to three significant figures, and does not represent perfect charge transfer.)

Long cycle life testing of 100,000 cycles was performed on the cell containing electrode composition 2.80. Figure 7 illustrates the cell's capacitance degradation versus cycle number (points plotted for every 1,000 cycles). The cell's capacitance degraded from 28.5 mF/cm$^2$ to 17.9 mF/cm$^2$ over the course of the test, a decrease of 37.0%. Note, however, that the largest drop (22.5% down to 22.1 mF/cm$^2$) occurred between cycle number 1 and 1,000, suggesting an initial "break-in" process occurred within the capacitor's first thousand cycles. Once the capacitor was "broken-in," the long cycle life capacitance only dropped by 14.5% over the course of the last 99,000 cycles.

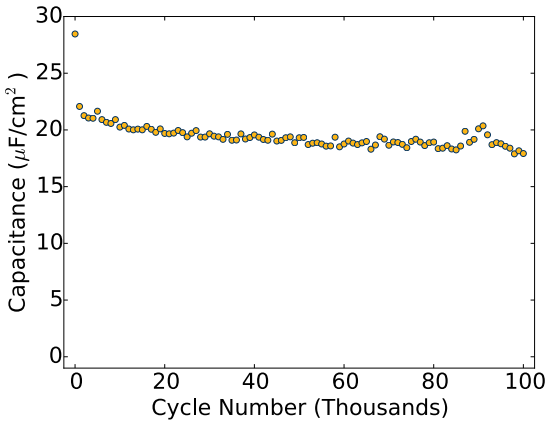


**Figure 7.** Long cycle life effects on cell capacitance

## 4. Conclusion

A high-current printable supercapacitor of composite carbon electrode composition employing gel polymer ionic liquid electrolyte has been shown to provide excellent discharge power to support trickle charging provided by micro-scale energy harvesters. This strong attribute promises to pair with micro-energy harvesting devices to meet the demands of high power devices, such as modern wireless radios, for applications in printed flexible wireless sensor nodes. The printing process employed can be rapidly scaled up for high-throughput manufacturing of printed energy storage to be integrated with MEMS device solutions.

## 5. Acknowledgments

The authors acknowledge the FlexTech Alliance for their sponsorship with award #RFP13-161.

## References

[1] Blystad LCJ, Halvorsen E, Husa S. 2010 *IEEE* **57** 908-19
[2] Liu J-Q, Fang H-B, Xu Z-Y, Mao X-H, Shen X-C, et al. 2008 *Microelectronics J.* **39** 802-6
[3] Wong ACW, Dawkins M, Devita G, Kasparidis N, Katsiamis A, King O, et al. 2013 *IEEE* **48** 186-98
[4] Crosthwaite J, Muldoon M, Dixon J, et al. 2005 *J. Chem. Thermodynamics* **37** 559-68
[5] Ho CC, Steingart D, Evans J, Wright P. 2008 *ECS Transactions* **16** 35-47
[6] Zhang H, Zhang W, Cheng J, Cao G, Yang Y. 2008 *Solid State Ionics* **179** 1946-50
[7] International standard: fixed electric double layer capacitors. IEC 62391-1; 2006
[8] Armand M, Endres F, MacFarlane DR, Ohno H, Scrosati B. 2009 *Nature Materials* **8** 621-9